

## Anthocyanins, Trimethylgossypentin Coumaric Acid, Quercetin-3'-O-glucoside of Roselle's Flower (*Hibiscus sabdariffa* L.) Molecular Docking on Bone Remodeling Biomarker: An In-silico study

Ida Bagus Narmada<sup>1,2</sup>, Sonya Liani Ramadanti<sup>1</sup>, Inggit Dwi Virgianti<sup>1</sup>, Putri Pramita Larasati<sup>1</sup>,  
I Gusti Aju Wahyu Ardani<sup>1,2</sup>, Ari Triwardhani<sup>1,2</sup>, Alida<sup>1,2</sup>, Ervina Restiwulan Winoto<sup>1,2</sup>,  
Alexander Patera Nugraha<sup>1,2\*</sup>, Viol Dhea Kharisma<sup>2,3</sup>,  
Tengku Natasha Eleena binti Tengku Ahmad Noor<sup>4,5</sup>

1. Department of Orthodontic, Faculty of Dental Medicine - Universitas Airlangga, Surabaya, East Java, Indonesia.
2. Dental Regenerative Research Group, Faculty of Dental Medicine, Airlangga University, Surabaya, East Java, Indonesia.
3. Division of Molecular Biology and Genetics, Generation Biology Indonesia Foundation, Gresik, Indonesia.
4. Military Dental Officer of Royal Medical and Dental Corps, Malaysian Armed Forces, Semenggo Camp, Kuching, Serawak, Malaysia.
5. Membership of Faculty of Dental Surgery, Royal College of Surgeon, Edinburgh University, United Kingdom.

### Abstract

By acting as mechanoreceptors, osteocytes can be stimulated by a mechanical orthodontic force to detect changes in blood flow in the bone canaliculi and respond by signaling osteoblasts and stimulating osteoclast development, which leads to bone resorption. Periodontal ligament (PDL) and alveolar bone renewal are necessary for optimal orthodontic tooth movement. *Hibiscus sabdariffa* flower may have the potential to improve alveolar bone regeneration in dentistry since it possesses anti-inflammatory, pro-osteogenic, pro-angiogenic, and anti-osteoclastogenic properties.

**Aim:** To evaluate the molecular docking of bioactive compounds in *H. sabdariffa* flower Anthocyanins, trimethylgossypentin-coumaric acid, Quercetin-3'-O-glucoside on bone remodeling biomarkers through an in silico study. The ADMET (absorption, distribution, metabolism, excretion, and toxicity) prediction of the chemical constituents of *H. sabdariffa* flowers was carried out.

Anthocyanins, 3,4,7'-trimethylgossypentin coumaric acid, and quercetin-3'-O-glucoside make up the chemical composition of the Roselle flower. The target proteins used were heat shock protein (HSP)-10, HSP-70, receptor activator nuclear kappa beta (RANK), RANK-Ligand (RANKL), osteoprotegerin (OPG), vascular endothelial growth factor (VEGF), fibroblast growth factor-2 (FGF-2), matrix metalloproteinase-9 (MMP-9), nuclear factor kappa beta (NFkB), tumor necrosis factor- $\alpha$  (TNF- $\alpha$ ), runt related transcription factor-2 (RUNX2), Osterix, nuclear factor associated T-cells1 (NFATc1), tartrate resistant acid phosphatase (TRAP), & collagen type 1a1 (Coll1A1) through molecular docking.

Quercetin-3'-O-glucoside in *H. sabdariffa* flower has a high binding affinity to osterix, FGF-2, and HSP-70 but not MMP-9 and TNF- $\alpha$ .

Quercetin-3'-O-glucoside in *H. sabdariffa* flower enhance bone regeneration through elevation of osteoblastogenesis but not osteoclastogenesis biomarker as documented in silico.

**Experimental article (J Int Dent Med Res 2023; 16(2): 522-530)**

**Keywords:** Medicine, dentistry, coumaric acid, quercetin, orthodontic.

**Received date:** 30 December 2022

**Accept date:** 25 January 2023

### Introduction

Malocclusion is the most common dental problem that people complain about and they

have the desire to perform orthodontic treatment. Malocclusion is an occlusion that deviates from the normal state, there is an irregularity of the teeth or the wrong placement of the dental arch outside the normal range.<sup>1</sup> The goal of orthodontic treatment is to improve the arrangement of the teeth and abnormal jaw relationships in order to achieve ideal occlusion, normal function, and good facial aesthetics, as well as to achieve harmonious facial shape, good masticatory relations and functions, and final result stability.<sup>2</sup> The use of orthodontic

#### \*Corresponding author:

Alexander Patera Nugraha DDS., MSc., MDS., PhD.  
Department of Orthodontics, Faculty of Dental medicine,  
Universitas Airlangga, Jl. Mayjen Prof. Dr. Moestopo 47,  
Postal Code 60132, Surabaya, Indonesia.  
E-mail: alexander-patera-nugraha@fkg.unair.ac.id

appliance puts pressure on the teeth so that the teeth move into the correct place, the movement of these teeth can stimulate an inflammatory response which is the beginning of bone remodelling.<sup>3</sup>

Bone continues to undergo a process of remodelling which is a complex process including bone resorption and formation. Bone remodelling requires the coordination of three types of cells, namely: osteocytes, osteoblasts, and osteoclasts. A mechanical force can induce osteocytes that act as mechanoreceptors to detect changes in blood flow in the bone canaliculi and respond via signal transmission to osteoblasts, then osteoblasts stimulate osteoclast differentiation and bone resorption.<sup>4</sup> When teeth movement, there is a tension and pressure on the bone surface. In the tension area, there will be a widening of the periodontal ligament which will stimulate increased cell replication so that it will increase collagen formation. The applied pressure will cause bone apposition and resorption. Tooth movement in orthodontic treatment responds to the periodontal tissue.<sup>5</sup>

Despite the effectiveness of current orthodontic treatment, there are a number of circumstances in which treatment efficiency can be increased by modulating osteoclast activity. One of them is the increasing incidence of root resorption during orthodontic treatment, or more commonly known as orthodontically induced inflammatory root resorption (OIRR).<sup>6</sup> Several studies suggest that 2-5% of orthodontic patients have severe OIRR (more than 5mm). Meanwhile, around 30-40% have moderate OIRR (more than 3mm) and 48-66% have mild OIRR (less than 2.5mm).<sup>7,8</sup>

*Hibiscus sabdariffa* L., family *Malvaceae* is a plant that is spread almost all over the world, including in Indonesia. *H. sabdariffa* flower petals are often consumed as tea and used as traditional medicine because *H. sabdariffa* flower petals contain vitamins, minerals and bioactive compounds, such as polyphenols, flavonoids, saponins, saponosides, tannins and anthocyanins. *H. sabdariffa* flower petals extract has a high antioxidant content derived from flavonoids, Gossypentin, Quercetin, Anthocyanins. *H. sabdariffa* flower petals extract has antihypertensive, antihyperlipidemic, antioxidant, anticancer, anti-inflammatory and anti-microbial abilities. so that it is often used as a treatment

material, besides that it is also easily available in various regions and countries.<sup>9</sup>

*H. sabdariffa* flower petals are a herbal plant that has the potential to heal alveolar bone injury in dentistry due to its anti-inflammatory and antibacterial properties. The unique composition of *H. sabdariffa* flower petals, which includes anthocyanins, polyphenols, niacin, riboflavin, ascorbic acid, calcium, iron, potassium, and magnesium, makes it highly helpful for human health. *H. sabdariffa* flower petals also contain delphinidin-3-sambubioside, which can decrease osteoclastogenesis by reducing the generation of inflammatory mediators.<sup>10</sup>

*H. sabdariffa* flower petals extract also modulates proinflammatory adipokine secretion and reduces ROS formation in hypertrophic cells, as Roselle containing Quercetin (Q) and Quercetin-3-O-glucuronide (Q3GA) has a greater capacity to decrease glucolipotoxicity-induced ROS generation than ascorbic acid or glucolipotoxic acid chlorogenic. Roselle flower extract Q and Q3GA reduced the release of cytokines such as leptin, tumor necrosis factor- $\alpha$  (TNF- $\alpha$ ), insulin growth factor-1 (IGF-1), interleukin-6 (IL-6), interleukin-1 (IL-1), and C-C motif ligand 2 (CCL2).<sup>11</sup> In a previous study of Quercetin in rats with acute pancreatitis, Quercetin may trigger an increase in IL-10 in the wound healing process. Quercetin (3,3',4',5,7-pentahydroxyflavone) is one of the active substances in the flavonoid class of the flavonol group which has very high free radical activity. Antioxidants from Quercetin compounds are able to trigger the collagen production and increase Vascular Endothelial Growth Factor (VEGF).<sup>12</sup> Furthermore, a previous study found that anthocyanin content could reduce the secretion of pro-inflammatory cytokines while increasing VEGF and fibroblast growth factor-2 (FGF-2), both of which are markers of neovascularization. Anthocyanins also act as antioxidants by increasing heat shock protein (HSP)-70 and ovalbumin while decreasing MDA. Anthocyanins were more efficient than tartaric acid and ascorbic acid in raising IL-10, VEGF, FGF-2, HSP-70, forkhead box P3 (Foxp3), ovalbumin, and lowering IL-1B, IL6, and tumor necrosis factor receptor (TNFR).<sup>13</sup> Therefore, this study aimed to evaluate the molecular docking of bioactive compounds in Roselle flower (*H. sabdariffa*) Anthocyanins, trimethylgossypentin coumaric acid, Quercetin-3'-O-glucoside to

osteoblastogenesis, osteoclastogenesis and angiogenesis/biomarkers through a bioinformatics approach, an *in silico* study.

## Materials and methods

### Preparation of the sample

Anthocyanins, 3,4,7'-trimethylgossypentin coumaric acid, and Quercetin-3'-O-glucoside were employed in this investigation as chemical compounds comprising Roselle. The target proteins employed in this investigation were NF- $\kappa$ B, TNF- $\alpha$ , RUNX2, osterix, NFATc1, TRAP, HSP-10, HSP-70, RANK, RANKL, OPG, VEGF, FGF-2, MMP-9, and COL1A1. We collected data on the 3D structure, visualization method, PDB ID, Resolution, weight, sequence length, and chain from the RCSB PDB database (<https://www.rcsb.org/>).<sup>14</sup>

### Prediction of Absorption, Distribution, Metabolism, Excretion, and Toxicity

The absorption, distribution, metabolism, excretion, and toxicity of the chemical components in *H. sabdariffa* were predicted by the Swiss ADME (<http://www.swissadme.ch/>) and ProTox-II ([https://tox.new.charite.de/protox\\_II/](https://tox.new.charite.de/protox_II/)). The degree of toxicity is often considered to be class IV or class V, and physicochemical properties, water solubility, and druglikeness are used to determine the ability of query compounds to be viable candidate drug molecules.<sup>15,16</sup>

### Virtual Examination

The capacity of *H. sabdariffa* flower petals to bind to target proteins comprised of nuclear factor kappa beta (NF- $\kappa$ B), tumor necrosis factor- $\alpha$  (TNF- $\alpha$ ), runt related transcription factor-2 (RUNX2), Osterix, nuclear factor associated T-cells1 (NFATc1), tartate resistant acid phosphatase (TRAP), heat shock protein (HSP)-10, HSP-70, receptor activator nuclear kappa beta (RANK), RANK-Ligand (RANKL), osteoprotegerin (OPG), vascular endothelial growth factor (VEGF), fibroblast growth factor-2 (FGF-2), matrix metalloproteinase-9 (MMP-9), & collagen type 1a1 (Coll1A1). Molecular docking simulations were used to predict the investigation's findings. Based on the value of binding affinity, molecular docking may be used to determine the kind of activity and pattern of molecular interactions of a ligand when it binds to the target protein. Depending on the research goals, the type of binding activity is either

inhibition or stimulator.<sup>17</sup>

### Interactions between ligands and proteins

The Discovery Studio 2016 version of the program was used to identify the sites and kinds of molecular interactions in this investigation. Chemical bond interactions including Van der Waals, hydrogen, hydrophobic, electrostatic, and pi are present in docked molecular complexes. The weak connections formed by the contacts play a part in triggering the target protein's activity.<sup>18</sup>

### Molecular Illustration

The PyMol 2.5 version application was used to pick the colors for the molecular docking 3D structure, which is displayed as clear surfaces, cartoons, sticks, and other objects. The Python-written program is used for structural selection or coloring of docked molecular complexes.<sup>19</sup>

### Analysis of the data

This study's data were examined descriptively by comparing the results to the standard. In silico study of *H. sabdariffa* to bind to target proteins consisting of NF- $\kappa$ B, TNF- $\alpha$ , RUNX2, Osterix, NFATc1, TRAP, HSP-10, HSP-70, RANK, RANKL, OPG, VEGF, FGF-2, MMP-9, Coll1A1 in this study were predicted through molecular docking simulations was analyzed by software. The drug-like molecule prediction was carried out using scfbio's drugdesign program (<http://www.scfbio-iitd.res.in/software/drugdesign/lipinski.jsp>). The PyRx 0.9.9 software version was utilized in this investigation to determine the binding capacity of chemicals found in Roselle to fifteen target proteins. The BIOVIA Discovery Studio 2017 edition software was used to examine the location and kind of chemical binding interaction.<sup>20</sup>

## Results

Thirteen target proteins were found in the database based on the predicted results of the ADMET substances anthocyanins, 3,4,7'-trimethylgossypentin coumaric acid, and quercetin-3'-O-glucoside from Roselle (Table 1). The two compounds are soluble and permit passage through the selectively permeable cell layer if they have a target in the cytoplasmic environment. Additionally, they meet several druglikeness criteria, and their toxicity level is



also low, being class 5 or low toxic (Table 2).

No	Name	Visualization Method	GDP ID	Resolution (Å)	Weight (kDa)	Sequence Length (mer)	Chain
1	NF-κB	NMR	2DBF	-	10.62	100	A
2	TNF-α	X-ray	1TNF	2.60	52.11	157	A
3	RUNX2	X-ray	6VGE	4.25	62.53	117	D
4	OSTERIX	NMR	6X46	-	14.35	121	A
5	NFATc1	NMR	1A66	-	27.33	178	A
6	TRAP	X-ray	1WAR	2.22	35.48	310	A
7	HSP-10	NMR	6MRD	3.82	27.33	178	C
8	HSP-70	X-ray	1S3X	1.84	42.75	382	A
9	RANK	X-ray	3URF	2.70	38.38	162	A
10	RANKL	X-ray	3URF	2.70	38.38	162	A
11	OPG	X-ray	3URF	2.70	38.38	162	A
12	VEGF	X-ray	2VPF	1.93	95.59	102	A
13	FGF-2	NMR	1BLA	-	17.35	155	A
14	MMP-9	X-Ray	1L6J	2.50	47.60	425	A
15	COLL1A1	NMR	2LLP	-	4.97	18	A

**Table 1.** Target protein from database.

Compounds	Physicochemical Properties	Water Solubility	Druglikeness	Toxicity
Anthocyanins (Compound A)	Formula: C <sub>15</sub> H <sub>11</sub> O <sup>+</sup> Weight: 207.25 g/mol Num. heavy atoms: 16 Num. scent. heavy atoms: 16 Csp3 Fraction: 0.00 Num. rotatable bonds: 1 Num. H-bond acceptors: 1 Num. H-bond donors: 0 Molar Refractivity: 66.06 TPSA: 13.14 <sup>2</sup>	Log S (ESOL): -4.01 Class: Moderately soluble Log S (Ali): -3.47 Class: Soluble Log S (SILICOS-IT): -5.32 Class: Moderately soluble	Lipinski: Yes Ghose: Yes Veber: Yes Egan: Yes Muege: No Bioavailability: 0.55	Predicted LD50: 2500 mg/kg Similarity: 71.67% Predicted Toxicity Class: 5 (Low Toxic)
3,4,7'-trimethylgossypentin coumaric acid (Compound B)	Formula: C <sub>19</sub> H <sub>16</sub> O <sub>3</sub> Weight: 164.16 g/mol Num. heavy atoms: 12 Num. scent. heavy atoms: 6 Csp3 Fraction: 0.00 Num. rotatable bonds: 2 Num. H-bond acceptors: 3 Num. H-bond donors: 2 Molar Refractivity: 45.13 TPSA: 57.53 <sup>2</sup>	Log S (ESOL): -2.02 Class: Soluble Log S (Ali): -2.27 Class: Soluble Log S (SILICOS-IT): -1.28 Class: Soluble	Lipinski: Yes Ghose: Yes Veber: Yes Egan: Yes Muege: No Bioavailability: 0.85	Predicted LD50: 2850 mg/kg Similarity: 100% Predicted Toxicity Class: 5 (Low Toxic)
Quarcetin-3'-O-glucoside (Compound C)	Formula: C <sub>27</sub> H <sub>19</sub> O <sub>12</sub> Weight: 463.37 g/mol Num. heavy atoms: 33 Num. scent. heavy atoms: 16 Fraction Csp3: 0.29 Num. rotatable bonds: 4 Num. H-bond acceptors: 12 Num. H-bond donors: 7 Molar Refractivity: 108.27 TPSA: 213.34 <sup>2</sup>	Log S (ESOL): -3.03 Class: Soluble Log S (Ali): -4.40 Class: Moderately soluble Log S (SILICOS-IT): -1.51 Class: Soluble	Lipinski: No Ghose: Yes Veber: No Egan: No Muege: No Bioavailability: 0.11	Predicted LD50: 5000 mg/kg Similarity: 97.30% Predicted Toxicity Class: 5 (Low Toxic)

**Table 2.** ADMET analysis of Anthocyanins, 3,4,7'-trimethylgossypentin coumaric acid, and Quarcetin-3'-O-glucoside.

According to the value of binding affinity created when quarcetin-3'-O-glucoside binds to all target proteins (Table 3), quarcetin-3'-O-glucoside has greater activity than anthocyanins and 3,4,7'-trimethylgossypentin coumaric acid. PyMol 2.5 version software with structural selection and staining was used to depict the docked molecular complexes in this investigation (Figure 1). The activity of the compound Quarcetin-3'-O-glucoside containing Roselle allows it to inhibit the regulation or decrease in protein activity consisting of TRAP, NFATc1, NF-κB, TNF-α, HSP-70, RANK, MMP-9, then

Quarcetin-3 activity '-O-glucoside from *H. sabdariffa* is also predicted to increase the activity consisting of RUNX2.

Protein	Autogrid						Affinity Binding (kcal/mole)		
	Center (Å)			Dimensions (Å)			A*	B*	C*
	X	Y	Z	X	Y	Z			
NF-κB	42,464	14,683	38,036	90,709	67,390	51,935	-6.1	-5.5	-6.5
TNF-α	19,968	49,675	39,930	80,739	58,243	58,256	-7.4	-5.9	-10.3
RUNX2	-50,956	39,759	-15,612	64,939	22,064	47,175	-5.2	-4.3	-5.9
OSTERIX	3,937	3,965	-46,055	66,285	36,739	27,656	-5.5	-4.4	-6.1
NFATc1	15,501	-7,918	1,696	68,461	53,410	57,713	-6.9	-6.3	-7.2
TRAP	68,304	-24,336	17,176	25,885	27,644	39,737	-6.6	-5.0	-7.0
HSP-10	-40,185	60,186	24,034	107,037	65,608	86,197	-7.0	-5.6	-7.2
HSP-70	17,346	32,160	13,643	63,552	62,888	65,835	-7.5	-6.5	-9.1
RANK	8,830	-0,536	17,364	47,953	57,932	51,740	-6.1	-5.3	-6.4
RANKL	8,830	-0,536	17,364	47,953	57,932	51,740	-6.1	-5.3	-6.4
OPG	-2,998	-3,671	23,788	95,207	98,636	77,806	-6.0	-5.0	-6.3
VEGF	-7,420	-1,430	-4,507	52,634	48,545	39,120	-5.9	-5.1	-6.1
FGF-2	-0,405	-0,177	0,022	43,945	45,327	38,543	-6.4	-5.3	-8.1
MMP-9	36,880	38,840	34,620	25,000	25,000	25,000	-7.4	-7.1	-8.0
COLL1A1	0,568	0,032	-0,246	49,934	17,523	22,589	-6.4	-5.5	-6.5

**Table 3.** The molecular docking results.

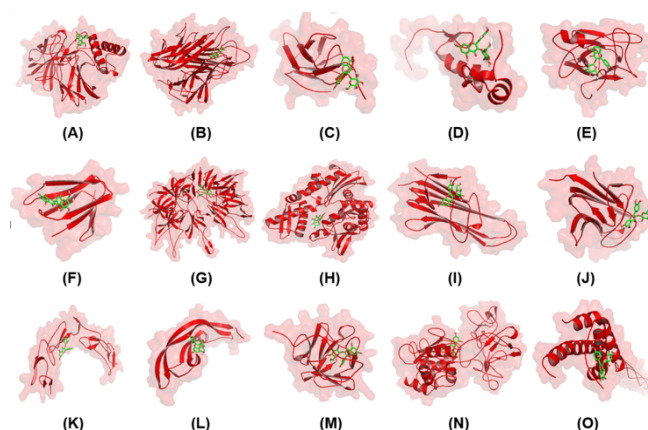


**Figure 1.** Molecular complex from docking simulation. (A) NF-κB\_Quarcetin-3'-O-glucoside, (B) TNF-α\_Quarcetin-3'-O-glucoside, (C) RUNX2\_Quarcetin-3'-O-glucoside, (D) OSTERIX\_Quarcetin-3'-O-glucoside, (E) NFATc1\_Quarcetin-3'-O-glucoside, (F) TRAP\_Quarcetin-3'-O-glucoside, (G) HSP-10\_Quarcetin-3'-O-glucoside, (H) HSP-70\_Quarcetin-3'-O-glucoside, (I) RANK\_Quarcetin-3'-O-glucoside, (J) RANKL\_Quarcetin-3'-O-glucoside, (K) OPG\_Quarcetin-3'-O-glucoside, (L) VEGF\_Quarcetin-3'-O-glucoside, (M) FGF-2\_Quarcetin-3'-O-glucoside, (N) MMP-9\_Quarcetin-3'-O-glucoside, (O) COLL1A1\_Quarcetin-3'-O-glucoside.

\*Information: A: Anthocyanins; B: 3,4,7'-trimethylgossypentin coumaric acid; C: Quarcetin-3'-O-glucoside.

The identification of molecular interactions and binding locations on the docked protein-

ligand complex (Figure 2) revealed that the binding of Quarcetin-3'-O-glucoside compounds to all target proteins resulted in non-covalent bond interactions comprising of Van der Waals, pi, and hydrogen (Table 4). Overall, weak binding interactions can lead to the creation of persistent ligand-protein complexes and generate activity responses on target proteins such as enhancement and inhibition.

Ligand-Protein	Chemical Interaction
NF- $\kappa$ B_Quarcetin-3'-O-glucoside	<b>Hydrogen:</b> Ser113, Leu143, Arg157, Asp121; <b>van der Waals:</b> Glu152, Glu160, His112, His144, Gly122; <b>Pi:</b> Ala156, Val61, Thr153, Val145, Lys149; <b>Unfavorable:</b> Thr146
TNF- $\alpha$ _Quarcetin-3'-O-glucoside	<b>Hydrogen:</b> Tyr115, Pro100, Ser99, Lys98, Ser99, Gln102, Gln103, Glu104; <b>van der Waals:</b> Trp114, Lys98, Gln102, Pro100, Cys101, Cys104, Trp114, Tyr115; <b>Pi:</b> Glu116; <b>Unfavorable:</b> Glu116
RUNX2_Quarcetin-3'-O-glucoside	<b>Hydrogen:</b> His129, Lys218, Asp222; <b>van der Waals:</b> Arg190, Gly192, Pro224, Thr220, Gly194, Arg225, Pro227; <b>Pi:</b> Val221, Arg193
OSTERIX_Quarcetin-3'-O-glucoside	<b>Hydrogen:</b> Ser76, Glu78, Gln79, Asp80; <b>van der Waals:</b> Leu48, Ile77, His57, Val59, His67; <b>Unfavorable:</b> Arg56, Gln58
NFATc1_Quarcetin-3'-O-glucoside	<b>Hydrogen:</b> Arg177, Ser175, Gln176, Cys174; <b>van der Waals:</b> Lys143, Thr145, Arg127, Tyr29, Asn128; <b>Pi:</b> Cys174, Lys125; <b>Unfavorable:</b> Ser129, Arg142
TRAP_Quarcetin-3'-O-glucoside	<b>Hydrogen:</b> His34, Val21, His33, Thr49, Glu36; <b>van der Waals:</b> Ile22, Gly23, Ser35, Gln47, Ile45, Leu44, Ala46, Ile55, His51; <b>Pi:</b> His51, Ile55, Ala46
HSP-10_Quarcetin-3'-O-glucoside	<b>Hydrogen:</b> Ile23, Gln45; <b>van der Waals:</b> Ala25, Glu37, Asn44, Lys84, Leu74, Thr82, Leu85, Lys9, Ile83, Asn44; <b>Pi:</b> Lys24, Lys42, Leu43
HSP-70_Quarcetin-3'-O-glucoside	<b>Hydrogen:</b> Arg261, Tyr41, Lys56, Glu268; <b>van der Waals:</b> Val59, Arg264, Thr14, Tyr15, Asp234, Gly202, Thr265, Gly203, His89; <b>Pi:</b> Phe68, Asp69, Glu231
RANK_Quarcetin-3'-O-glucoside	<b>Hydrogen:</b> His189, Arg191; <b>van der Waals:</b> Asp190, Tyr188, Asn171, Thr173, Trp187, Phe201, Gly204, Asn203, Ser202, Ser185, Ser186; <b>Pi:</b> His189, Arg191
RANKL_Quarcetin-3'-O-glucoside	<b>Hydrogen:</b> His189; <b>van der Waals:</b> Asp190, Tyr188, Asn171, Thr173, Ser202, Ser185; <b>Pi:</b> His189, Arg191
OPG_Quarcetin-3'-O-glucoside	<b>Hydrogen:</b> Glu116, His80, Arg82, Cys84; <b>van der Waals:</b> Pro64, Ser63, Gln70, Tyr49, Asp51, Asn81, Glu85; <b>Pi:</b> Val83; <b>Unfavorable:</b> Lys73
VEGF_Quarcetin-3'-O-glucoside	<b>Hydrogen:</b> Gln37, Asp41, Ser95, Phe96, Asn75; <b>van der Waals:</b> Arg56, Leu97, Glu42, Glu38; <b>Pi:</b> Pro40, Tyr39
FGF-2_Quarcetin-3'-O-glucoside	<b>Hydrogen:</b> Ser152, Lys30, Asn113, His21; <b>van der Waals:</b> Asn111, Met151, Pro13, Pro150, Leu149, Phe26, Glu105, Ala20, Gly17, Gly19; <b>Pi:</b> Leu107, Phe21
MMP-9_Quarcetin-3'-O-glucoside	<b>Hydrogen:</b> Thr96, Asn38, Arg95, Tyr48; <b>van der Waals:</b> Thr37, Met94, Arg98, Pro97, Gly186, Asp185, Tyr52, Leu187, Arg51, Leu44; <b>Pi:</b> Leu39, Glu47
COL1A1_Quarcetin-3'-O-glucoside	<b>Hydrogen:</b> Ser71, Ala57, Leu67; <b>van der Waals:</b> Gln101, Gln58, Ile72, Ala68, Ala60, Pro66, Pro69, Gly70; <b>Pi:</b> Ala57, Leu67

**Table 4.** Molecular interaction analysis result between Quarcetin-3'-O-glucoside with fifteen targeted protein.

## Discussion

The binding mechanism of Anthocyanins, 3,4,7'-trimethylgossypentin coumaric acid, and Quarcetin-3'-O-glucoside with proteins was predicted using molecular docking simulations. The docking program utilized in this work was PyRx 0.9.9. By calculating the amount of ligand binding capacity to the protein domain based on the binding affinity value of the stable ligand-

protein complex, the simulation aims to produce negative energy.<sup>21,22</sup> When a protein interacts with a ligand, binding affinity is produced; this energy is created via a reversible process at constant temperature and pressure in accordance with thermodynamic laws.<sup>23</sup> The target protein's ligand's binding is guided by the grid in the docking simulation.<sup>24</sup> There are tension and compression in the bone surface as teeth move. There will be an expansion of the periodontal ligament in the stress area, which will drive greater cell reproduction and collagen creation. Because of changes in blood flow, forces applied to the teeth create changes in the macroenvironment around the periodontal ligament, resulting in the release of inflammatory mediators such as cytokines, growth factors, neurotransmitters, colony-stimulating factors, and arachidonic metabolism. The synchronization of three processes is required for bone remodeling: osteogenic, osteoclastogenic, and angiogenic. Several markers that play a role in the inflammatory process used in this in silico test are NF $\kappa$ B and TNF- $\alpha$ , in the osteogenic process, namely RUNX2 and osterix, in the osteoclastogenic process, namely NFATc1, TRAP, MMP-9 and COLL1A1 and in the angiogenic process, the markers tested are VEGF and FGF-2. And besides having an impact on the 3 processes above, the Quarcetin in *H. sabdariffa* flower petals has an effect antioxidant through an increase in HSP-70 and HSP-10.<sup>25</sup>

TNF- $\alpha$  is a proinflammatory cytokine produced by a variety of cells, including macrophages and periodontal ligament cells. TNF- $\alpha$  is triggered by exogenous, endotoxin, and pathogenic stimulation. TNF- $\alpha$  levels were found to be increased in the gingival crevicular fluid (GCF) during orthodontic tooth movement. TNF- $\alpha$  activates the IKK complex which then phosphorylates I $\kappa$ B $\alpha$ . I $\kappa$ B $\alpha$  is a protein that binds to NF $\kappa$ B in the cytosol, so that NF $\kappa$ B is inactive and remains in the cytosol. Phosphorylated I $\kappa$ B $\alpha$  is degraded in the proteasome, causing translocation of cytosolic NF $\kappa$ B towards the nucleus and triggers osteoclastogenesis and inhibits osteoblast function.<sup>26</sup>

Nuclear Factor of Activated T-cells 1 (NFATc1) is a major regulator of the receptor activator of the Nuclear Factor Kappa Beta Ligand (RANKL), which induces osteoclast differentiation and plays an important role in osteoclast fusion and activation through

osteoclast upregulation of various genes responsible for osteoclast attachment, migration, acidification, inorganic degradation, and bone organic matrix.<sup>9</sup> The increase in NFATc1 expression on the pressure side was greater than on the tension side, indicating that applying orthodontic force on the pressure side increased the expression of RANKL, which further increased osteoclastogenesis, resulting in increased bone resorption and orthodontic tooth movement, followed by remodeling of the alveolar bone and periodontal ligament.<sup>27</sup>

Tartrate-Resistant Acid Phosphatase (TRAP) is one of six acid phosphatase isozymes, the fifth of which is obtained from osteoclasts, erythrocytes, and platelets. TRAP expression is a component of macrophage-osteoclast cell interaction and serves as an excellent marker for bone resorption and osteoclast activity.<sup>18</sup> TRAP is greatly impacted by orthodontic forces on both the pressure and tensile sides; according to study, the quantity of TRAP increases with orthodontic tooth movement as compared to no orthodontic force applied.<sup>28</sup>

Nuclear factor  $\kappa$ B ligand receptor activator (RANKL), its cellular receptor, NF- $\kappa$ B receptor activator (RANK), and decoy receptor osteoprotegerin (OPG) have been found to play important roles in the regulation of bone metabolism. Periodontal remodeling on the compression side. Under compressive strain, periodontal ligament (PDL) cells produce interleukin-1 (IL-1) and IL-6 (1), which act in an autocrine and paracrine manner to regulate nuclear factor B ligand receptor activator (RANKL) and matrix metalloproteinase (MMP) expressed by PDL cells and osteoblasts. MMPs generated by osteoblasts dissolve the unmineralized bone's surface osteoid layer, whereas MMPs produced by PDL cells damage their extracellular matrix. RANKL promotes the creation and function of osteoclasts from mononuclear precursor cells, which reach the bone surface and destroy the mineral matrix. MMP expression by osteocytes close to the bone surface is regulated by alveolar bone deformation.<sup>26,27</sup>

Because of VEGF's biological roles, such as increasing vascular permeability and aiding chemotaxis, blood arteries proximal to hyalinized tissue can offer many new cell types to degraded tissues, including fibroblasts, mesenchymal cells,

macrophages, and multinuclear giant cells. At the pull location, VEGF expression was also seen in PDL cells and osteoblasts. Compression and Tensile stresses stimulate the formation of VEGF and osteoblasts. In addition to stimulating bone healing, VEGF also promotes angiogenesis and bone remodeling.<sup>29,30</sup> Along with Notch signaling, which may convert nearby cells into stem cells and lead to VEGF receptor expression, VEGF can cause endothelial cell polarization and contribute to cell formation determination. FGF-2 is also important in angiogenesis; FGF ligands or their unique tissue-specific expression patterns control endothelial cell protrusion. Endothelial cell FGF-2 deficiency causes abnormalities in endothelial cell integrity, while FGF-2 can stimulate endothelial cell proliferation and vascular healing after damage.<sup>29,31</sup>

RUNX2 plays a critical function in osteoblast development by binding mesenchymal stem cells to osteoblast derivatives and favorably impacting the stage of osteoblast differentiation. RUNX2 is involved in the expression of bone matrix collagen type 1 genes, osteopontin, bone sialoprotein, and osteocalcin during the differentiation process of osteoblasts.<sup>32</sup> Osterix was discovered to be a bone morphogenic protein-2 (BMP2)-induced gene in mouse pluripotent mesenchymal cells that encodes a transcription factor highly selective for osteoblasts. Osterix is also expressed in pre-hypertrophic chondrocytes at low levels. On days 10 and 14 following fracture, osteoblasts in the fracture callus expressed Osterix. Osterix is frequently expressed on osteoblasts that regenerate at fracture sites.<sup>33</sup> The BMP2 signaling pathway includes a target for activating RUNX2 and, as a result, Osterix expression. RUNX2 also controls important osteoblast-specific downstream genes including as COL1A1, osteopontin, and osteocalcin, which govern the phenotypic and function of osteoblasts in skeletogenesis and are translated into matrix proteins. RUNX2 regulates osterix, which in turn regulates COL1A1, osteopontin, and osteocalcin.<sup>34</sup> Osterix is also involved in the development of preosteoblasts into mature osteoblasts. Preosteoblasts at this stage express early osteoblast marker genes such as ALP, which controls the phenotypic and function of osteoblasts throughout skeletogenesis and is translated into matrix proteins.



## Conclusions

According to molecular docking studies, Quarcetin-3'-O-glucoside in *H. sabdariffa* flower enhance bone regeneration through elevation of osteoblastogenesis but not osteoclastogenesis biomarker as documented in silico. More research is needed to evaluate the mechanical, biological, and chemical aspects of the combined bioactive component of *H. sabdariffa* flower petals *in vitro*, *in vivo*, and clinical trial settings.

## Declaration of Interest

The authors there is not conflict of interest in the manuscript.

## Acknowledgments

This research was funded by Penelitian Dasar Unggulan Perguruan Tinggi (PDUPT) fiscal year of 2022 by Ministry of Education Indonesia with appointment number 1004/UN3/2022 and 189/E5/PG.02.00.PT/2022, 851//UN3.15/PT/2022.

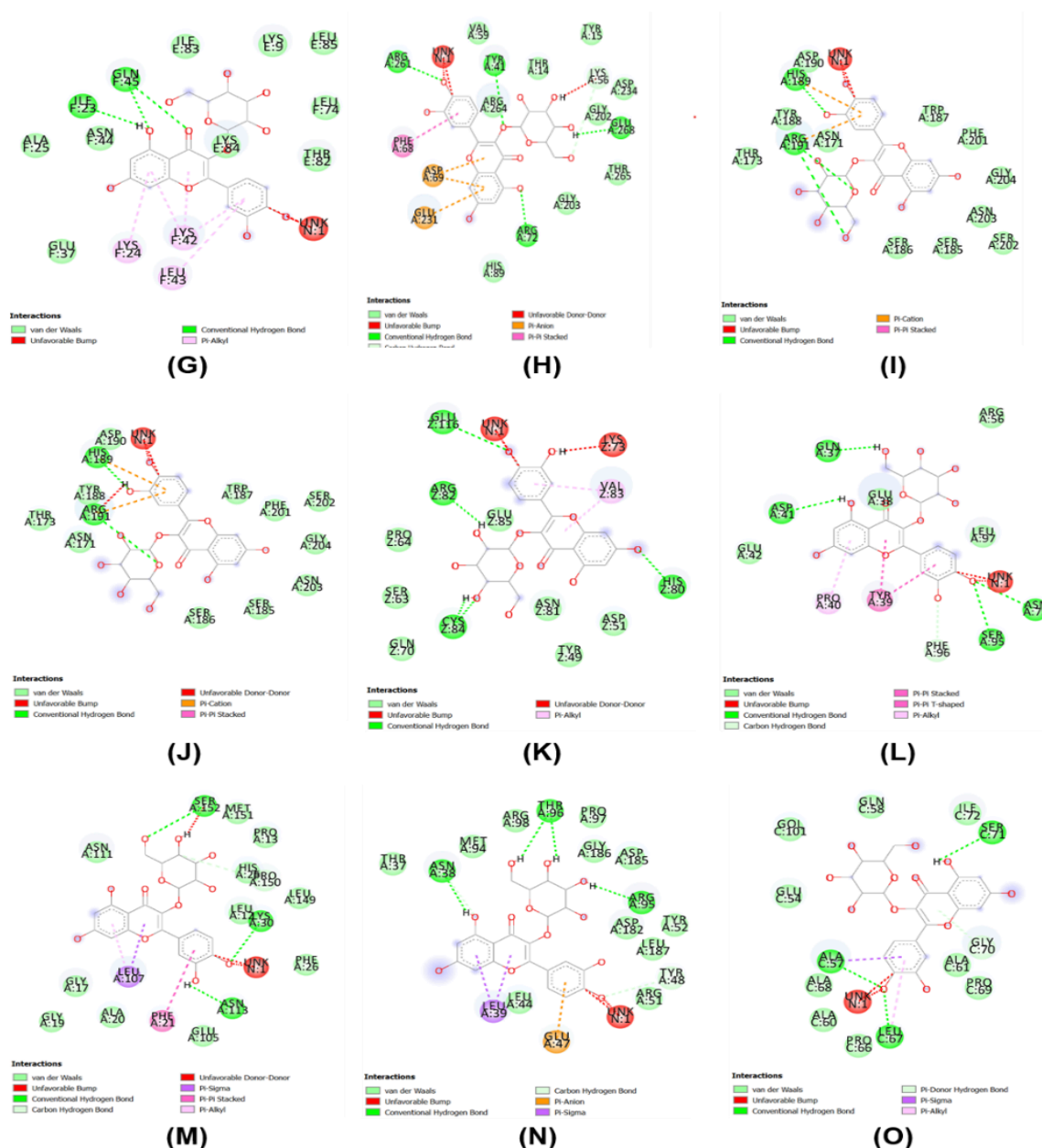


**Figure 2.** Position and kinds of chemical bond interactions in the ligand-protein complex are seen in 2D. from a docking simulation, a molecular complex. (A) NF- $\kappa$ B\_ Quarcetin-3'-O-glucoside, (B) TNF-

$\alpha$ \_Quarcetin-3'-O-glucoside, (C) RUNX2\_Quarcetin-3'-O-glucoside, (D) OSTERIX\_Quarcetin-3'-O-glucoside, (E) NFATc1\_Quarcetin-3'-O-glucoside, (F) TRAP\_Quarcetin-3'-O-glucoside, (G) HSP-10\_Quarcetin-3'-O-glucoside, (H) HSP-70\_Quarcetin-3'-O-glucoside, (I) RANK\_Quarcetin-3'-O-glucoside, (J) RANKL\_Quarcetin-3'-O-glucoside, (K) OPG\_Quarcetin-3'-O-glucoside, (L) VEGF\_Quarcetin-3'-O-glucoside, (M) FGF-2\_Quarcetin-3'-O-glucoside, (N) MMP-9\_Quarcetin-3'-O-glucoside, (O) COLL1A1\_Quarcetin-3'-O-glucoside.

## References

- Ardani IGAW, Willyanti I, Narmada IB. Correlation between vertical components and skeletal Class II malocclusion in ethnic Javanese. *Clin Cosmet Invest Dent*. 2018;10:297-302. Published 2018 Dec 19. doi:10.2147/CCIDE.S188414
- Ardani IGAW, Budipramana M, Rachmawati E, et al. COL1A1 and FGFR2 Single-Nucleotide Polymorphisms Found in Class II and Class III Skeletal Malocclusions in Javanese Population. *Eur J Dent*. 2023;17(1):183-190. doi:10.1055/s-0042-1744371
- Sitasari PI, Narmada IB, Hamid T, Triwardhani A, Nugraha AP, Rahmawati D. East Java green tea methanolic extract can enhance RUNX2 and Osterix expression during orthodontic tooth movement in vivo. *J Pharm Pharmacogn Res*. 2020;8(4):290-8.
- Prahasanti C, Nugraha AP, Kharisma VK, Ansori ANM, Ridwan DR, Putri TSP, Ramadhani NF, Narmada IB, Ardani IGAW, Noor TNEBA. A bioinformatic approach of hydroxyapatite and polymethylmethacrylate composite exploration as dental implant biomaterial. *J Pharm Pharmacogn Res*. 2021;9(5):746-54.
- Ernawati DS, Nugraha AP, Narmada IB, Ardani IGAW, Hamid T, Triwardhani A, et al. The Number of Osteoblast and Osteoclast during Orthodontic Tooth Movement after Preconditioned Gingiva Mesenchymal Stem Cell Allogeneic Transplantation in vivo. *J Int Dent Med Res*. 2022;15(3):1069-77.
- Salikha K, Narmada IB, Alida, Nugraha AP, Sari AF, Riawan W, et al. Anti-inflammatory effect of caffeic acid phenethyl ester supplementation on TNF- $\alpha$  and NF- $\kappa$ B expressions throughout experimental tooth movement in vivo. *J Pharm Pharmacogn Res*. 2022;10(6):1037-45.
- Hartsfield JK, Everett ET, Al-Qawasmi RA. Genetic factors in external apical root resorption and orthodontic treatment. *Crit Rev Oral Biol Med*. 2004;15(2):115-22.
- Kalra S, Gupta P, Tripathi T, Rai P. External apical root resorption in orthodontic patients: molecular and genetic basis. *J Fam Med Prim Care*. 2020;9(8):3872.
- Riaz A, Rasul A, Hussain G, Zahoor MK, Jabeen F, Subhani Z, et al. Astragalin: A Bioactive Phytochemical with Potential Therapeutic Activities. *Adv Pharmacol Sci*. 2018;2018.
- Idrus E, Tsary DA, Setiadi DS, Jesslyn, Calina NE, Halim VA, et al. Inhibition of alveolar bone destruction by roselle extract (*Hibiscus sabdariffa* L.). *J Int Dent Med Res*. 2020;13(3):830-5.
- Herranz-López M, Olivares-Vicente M, Rodríguez Gallego E, Encinar JA, Pérez-Sánchez A, Ruiz-Torres V, et al. Quercetin metabolites from *Hibiscus sabdariffa* contribute to alleviate glucolipotoxicity-induced metabolic stress in vitro. *Food Chem Toxicol*. 2020;144:111606.
- Peravali RK, Jayade B, Joshi A, Shirganvi M, Bhaskar Rao C, Gopalkrishnan K. Osteomyelitis of Maxilla in Poorly Controlled Diabetics in a Rural Indian Population. *J Maxillofac Oral Surg*. 2012;11(1):57-66.
- Narmada IB, Putri PD, Lucynda L, Triwardhani A, Ardani IG, Nugraha AP. Effect of caffeic acid phenethyl ester provision on fibroblast growth factor-2, matrix metalloproteinase-9 expression, osteoclast and osteoblast numbers during experimental tooth movement in wistar rats (*Rattus norvegicus*). *Eur J Dent*. 2021;15(02):295-301.
- Titiek B, Nugraha APN, Hidayati NN, Kharisma, Viol Dhea, Nugraha, Albertus Putera Noor TNEBTA. Computational study of Cu 2+, Fe 2+, Mn 2+, Mn 3+, Fe 3+, CrO4 2-, Si 4+, and Hg + binding sites identification on cytokines to predict dental metal allergy: An in silico study. *J Pharm Pharmacogn Res*. 2022;10(4):687-94.
- Daina A, Michielin O, Zoete V. SwissADME: a free web tool to evaluate pharmacokinetics, drug-likeness and medicinal chemistry friendliness of small molecules. *Sci Reports*. 2017;7(1):1-13.
- Banerjee P, Eckert AO, Schrey AK, Preissner R. ProTox-II: a webserver for the prediction of toxicity of chemicals. *Nucleic Acids Res*. 2018;46(W1):W257-63.
- Nugraha AP, Ardani IGAW, Sitalaksmi RM, et al. Anti-Peri-implantitis Bacteria's Ability of Robusta Green Coffee Bean (Coffea Canephora) Ethanol Extract: An In Silico and In Vitro Study [published online ahead of print, 2022 Sep 8]. *Eur J Dent*. 2022;10.1055/s-0042-1750803. doi:10.1055/s-0042-1750803
- Ardani IGAW, Patera Nugraha A, Suryani MN, Hafidz R, Pamungkas P, et al. Molecular docking of polyether ether ketone and nano-hydroxyapatite as biomaterial candidates for orthodontic mini-implant fabrication. *J Pharm Pharmacogn Res*. 2022;10(4):676-86.
- Luqman A, Kharisma VD, Ruiz RA, Götz F. In silico and in vitro study of Trace Amines (TA) and Dopamine (DOP) interaction with human  $\alpha$ 1-adrenergic receptor and the bacterial adrenergic receptor QseC. *Cell Physiol Biochem*. 2020;54(5):888-98.
- Nugraha AP, Sibero MT, Nugraha AP, et al. Anti-Periodontopathogenic Ability of Mangrove Leaves (*Aegiceras corniculatum*) Ethanol Extract: In silico and in vitro study. *Eur J Dent*. 2023;17(1):46-56. doi:10.1055/s-0041-1741374
- Nugraha AP, Rahmadhani D, Puspitaningrum MS, Rizqianti Y, Kharisma VD, and Ernawati DS. Molecular docking of anthocyanins and ternatin in Clitoria ternatea as coronavirus disease oral manifestation therapy. *J Adv Pharm Technol Res*. 2021;12(4):362.
- Kharisma VD, Utami SL, Rizky WC, Dings TGA, Ullah ME, Jakhmola V, Nugraha AP. Molecular docking study of Zingiber officinale Roscoe compounds as a mumps virus nucleoprotein inhibitor. *Dent. J. [Internet]*. 2023;56(1):23-9. Available from: <https://e-journal.unair.ac.id/MKG/article/view/35122>
- Pinzi L, Rastelli G. Molecular Docking: Shifting Paradigms in Drug Discovery. *Int J Mol Sci*. 2019;20(18):4331.
- Nugraha AP, Ardani IGAW, Sitalaksmi RM, et al. Anti-Peri-implantitis Bacteria's Ability of Robusta Green Coffee Bean (Coffea Canephora) Ethanol Extract: An In Silico and In Vitro Study [published online ahead of print, 2022 Sep 8]. *Eur J Dent*. 2022;10.1055/s-0042-1750803. doi:10.1055/s-0042-1750803
- Herniyati, Harmono H, Devi LS, Hernawati S. Cellular Analysis In Orthodontic Tooth Movement Post Robusta Coffee Extract Administration. *J Int Dent Med Res* 2019;12(3):969-976.
- Osta B, Benedetti G, Miossec P. Classical and paradoxical effects of TNF- $\alpha$  on bone homeostasis. *Front Immunol*. 2014;5:48.
- Krishnan V, Davidovitch Z. Biological Basis of Orthodontic Tooth Movement. *Biol Mech Tooth Mov*. 2021;1-15.
- Dorchin-Ashkenazi H, Ginat-Koton R, Gabet Y, Klein Y, Chaushu S, Dorchin H, et al. The Balance between Orthodontic Force and Radiation in the Jawbone: Microstructural, Histological, and Molecular Study in a Rat Model. *Biol* 2021;10(11):1203.
- Inayati F, Narmada IB, Ardani IGAW, Nugraha AP, Rahmawati D. Post oral administration of epigallocatechin gallate from *Camelia sinensis* extract enhances vascular endothelial growth factor and fibroblast growth factor expression during orthodontic



- tooth movement in wistar rats. J Krishna Inst Med Sci Univ. 2020;9(1):58–65.
30. Miyagawa A, Chiba M, Hayashi H, Igarashi K. Compressive Force Induces VEGF Production in Periodontal Tissues. J Dent Res. 2009;88(8):752–6.
  31. Seo HS, Lee DJ, Chung JH, Lee CH, Kim HR, Kim JE, et al. Hominis Placenta facilitates hair re-growth by upregulating cellular proliferation and expression of fibroblast growth factor-7. BMC Complement Altern Med. 2016;16(1):1–8.
  32. Deshpande S, James AW, Blough J, Donneys A, Wang SC, Cederna PS, et al. Reconciling the effects of inflammatory cytokines on mesenchymal cell osteogenic differentiation. J Surg Res. 2013 Nov 1;185(1):278–85.
  33. Vongkamolchoon S, Sinha SP, Liao YF, Chen YR, Huang CS. The impact of a surgery-first approach on oral health-related quality of life. Int J Oral Maxillofac Surg. 2021 Oct 1;50(10):1336–41.
  34. Choi JW, Shin S, Lee CY, Lee J, Seo HH, Lim S, et al. Rapid Induction of Osteogenic Markers in Mesenchymal Stem Cells by Adipose-Derived Stromal Vascular Fraction Cells. Cell Physiol Biochem. 2017;44(1):53–65.